Supporting Information

Ji *et al.* 10.1073/pnas.0806499105

SI Text

Orai1 Molecules Produce Independent Excess Noise during Bleaching Steps. As shown in Fig. 1 *D* and *E*, the fluorescence intensity of puncta fluctuates significantly. We now consider the details of this noise and argue that it is primarily caused by independent fluctuations in successively bleached EGFP molecules with little contribution from instrument noise, background noise, or photon-counting statistics. Cells were fixed before analysis, so there is no diffusion in and out of the field of analysis. The fluorescence intensity we report throughout our single-molecule analysis is the number of photons detected on a 25-pixel area of the EMCCD during a 200-ms counting period. We determined the variance of the photon count signals seen in the four bleaching steps of puncta formed by Orai1 singles (Fig. S3). As expected, if each fluorescent molecule is an independent noise source, the variance depends, in an approximately linear fashion, on the number of remaining fluorescent Orai1 molecules. The variance decreases ≈4,000 photons^2 per molecule lost. If Orai1 molecules were a steady source of fluorescence, the measurement noise from photon-counting statistics would follow the Poisson distribution with a variance equal to the mean. Later we show that the mean photon count per molecule is less than 200 photons, so Poisson counting statistics accounts for less than 5% of the observed variance. The basal variance when all Orai1 molecules are bleached is also small, so the major part of the observed variance is probably the reported rapid, on-and-off blinking of EGFP, corresponding to its transition between the excited and dark states (1). Similar results were obtained with cells transfected with the other Orai1 constructs.

Fluorescence Intensity of a Single EGFP. To determine the number of molecules in larger aggregates, we wanted to know the brightness of a single EGFP in our measurement apparatus. When Orai1 four-tandems were co-expressed with STIM1 in HEK293 cells, their bleaching usually exhibited a single step, as we saw in Fig. 1*D* in the main text. The amplitude profile of such steps was fitted with a Gaussian function, with a peak at 183 ± 7 photons (n = 104, Fig. S5*A*). As most of our experiments were conducted using the same recording parameters, this should correspond to the unitary fluorescence intensity of one EGFP molecule in our experimental setup in fixed cells. For the same bleaching measurements with four-tandems, the lifetime before bleaching was approximately exponentially distributed as expected, with an exponential time constant of 15.9 ± 3.3 s. From this we can calculate that, on average, we collect 14,500 photons (183 × 15.9 / 0.2) from one GFP fluorophore before it bleaches.

When Orai1-EGFP singles were co-expressed with STIM1 in HEK293 cells, their bleaching usually exhibited four steps (Fig. 1*D*). Unexpectedly, the first two steps were larger (>200 photons) than the latter two (<200 photons, Fig. S5*B*). This was not reported in previous studies (2, 3). It suggests a small increase in quantum yield when four functional EGFPs are present in one assembled CRAC channel. The mean intensity of puncta that bleached in four steps was 760 ± 35 photons (n = 60), which is naturally the sum of the four steps in Fig. S5*B*. Dividing this by four gives an estimate of 190 photons per EGFP, similar to the previous one.

Counting CRAC Channels Optically. Finally, we can use the brightness of a single EGFP to count CRAC channels. We consider how many CRAC channels are aggregated in clusters when intracellular Ca^{2+} stores become depleted. This number ultimately determines the amplitude and range of Ca^{2+} microdomains generated by the Ca^{2+} entry.

As reported in our previous work and that of others (4–6), when the ER Ca^{2+} was depleted by incubation with TG, fluorescent Orai1 assembled into bright aggregates. They were readily seen with TIRF microscopy at 1/100 the gain used for single-molecule imaging (Fig. S2*B*). The light intensity per bright cluster had a surprisingly narrow intensity distribution. Within the same cell, the SD in fluorescence intensity among the different clusters was less than 8% of the average intensity (n = 4 cells and 158 clusters), indicating that these Orai1 molecules assemble in some stereotyped and uniform fashion. Measured in four cells transfected with Orai1 singles, the mean fluorescence density in clusters was 4,607 ± 458 counts per pixel or ≈16,000 photons per pixel (see *Methods*). Translating this brightness yields ≈88 (i.e., 16,000/180) Orai1 molecules or 22 CRAC channel complexes per pixel in a cluster after ER depletion. Because the area of single clusters is 1.5 ± 0.4 μm^2 (or 58 ± 15 pixels), the number of aggregated CRAC channel complexes in each cluster is ≈1,300.

For completeness, we now use the following statistical properties of our preparation to scale these numbers: each pixel is 160 × 160 nm, the summed area of clusters within one TIRF footprint is 58 ± 11 μm^2, the TIRF footprint is 193 ± 14 μm^2 per cell, and the plasma membrane area of a whole cell is ≈1,500 μm^2. The latter membrane area derives from the membrane capacitance seen with electrophysiology (≈15 pF), assuming the conventional conversion factor 100 μm^2/pF. This would mean that each CRAC channel consisting of four Orai1 molecules occupies an area of 34 × 34 nm ($160/22^{0.5}$) in the cluster, that there are 48,000 channels per footprint, and that, if the rest of the cell membrane is like the footprint, there are 370,000 channels per cell. Because we estimate that possibly 20% of the Orai1 molecules lack fluorescent EGFP, the total number of channels may be slightly underestimated.

Methods ***Construction of plasmids.*** The Orai1 cDNA was PCR amplified from pOrai1-EGFP with the flexible linker GGSGGTGGSLHPGLSPGLLPLHPASI (Fig. 1*A*) inserted immediately upstream of the N terminus of Orai1. The cDNA sequence, flanked by an XhoI site at the N terminus and a SalI at the C terminus, was inserted into pEGFP-N1 or monomeric mKO-N1 vector (MBL International) digested with XhoI and SalI to produce EGFP- or mKO-labeled Orai1 singles. To produce an EGFP-labeled Orai1 two-tandem, the Orai1 fragment with the linker sequence was digested with XhoI and BamH I, and then inserted into the Orai1 plasmid digested with SalI and BamH I. Similar methods were used to generate Orai1 three-tandems and four-tandems. STIM1-mOrange was constructed as previously described (5). The C terminus of STIM1 (residues 237–685) was amplified from pHluorin–STIM1 using the NheI and the SalI sites and tagged with either EGFP or mCherry by insertion into the appropriate vector digested with NheI and SalI (Fig. 1*B* in the main text). Human Orai1 cDNA tagged with 3× FLAG tag was subcloned into pCTAP vector (Stratagene) to obtain the Orai1–3× FLAG-SBP-CBP vector.

Cell culture, transfection, and stable cell line construction. HEK293 cells were cultured as described previously (5). STIM1 and the different Orai1 vectors were always mixed in a 5:1 weight ratio, containing a total amount of 3.2 μg of DNA. Cells were transfected with Lipofectamine 2000 (Invitrogen) following the manufacturer's instructions, and were dropped onto low-

autofluorescence coverslips (Fisher Scientific). Cells in Figs. 1, 2, 4 *B* and *C*, S3, S5, and S6 were transfected for only 2–5 h. Cells in Figs. 3, 4*A*, S1, S2, S4, and S7 were transfected for 16–30 h. For TIRF microscopy on fixed cells, the cells were taken at 2–5 h after transfection, fixed for 15 min with 4% paraformaldehyde (Sigma-Aldrich) in PBS, rinsed in PBS, and placed in PBS solution before the experiment (7). For stable cell line construction, cells were transfected with linear PEI (Polysciences) according to the manufacturer's instructions. WT control cells and cells transfected with Orai1–3× FLAG-SBP-CBP were processed with cytotoxic pressure screen (2,000 μg/ml G418, Sigma) for 10 days until all control cells died. The living healthy cells stably expressing the Orai1–3× FLAG-SBP-CBP gene were collected and cultured for experiments.

Electrophysiology. Patch–clamp experiments were conducted at room temperature using the whole-cell recording configuration, as described (8). In brief, high-resolution current recordings were acquired using an EPC-10 amplifier (HEKA). After establishing the whole-cell configuration, voltage ramps lasting 50 ms and spanning –100 to +100 mV were delivered from a holding potential of 20 mV every 2 seconds over a period of 300–500 s. All voltages were corrected for a liquid-junction potential of 10 mV. Currents were filtered at 2.9 kHz and digitized at a rate of 20 kHz. Capacity currents were determined and corrected before each voltage ramp. The amplitude of the current recorded at –80 mV was used to monitor the development of CRAC current (I_{CRAC}).

Single-cell $[Ca^{2+}]_i$ measurements. Cells were preincubated with 6 μM fura-2/AM at room temperature for 30 min in standard Ringer solution. $[Ca^{2+}]_i$ was measured by dual-wavelength excitation (340/380 nm) photometry on an inverted microscope (Olympus IX71, Olympus) equipped with a polychromatic xenon light source (TILL Photonics). The emission was collected at 510 ± 5 nm with a photodiode controlled by the TILL photometry system and the X-Chart extension of Pulse software (HEKA). $[Ca^{2+}]_i$ was calculated from the background-corrected fluorescence ratio R (9). Calibration parameters of R_{min} (0.145), R_{max} (4.069), and K_{eff} (3.90 μM) were determined previously (10).

1. Dickson RM, Cubitt AB, Tsien RY, Moerner WE (1997) On/off blinking and switching behaviour of single molecules of green fluorescent protein. *Nature* 388:355–358.
2. Kohout SC, Ulbrich MH, Bell SC, Isacoff EY (2008) Subunit organization and functional transitions in Ci-VSP. *Nat Struct Mol Biol* 15:106–108.
3. Ulbrich MH, Isacoff EY (2007) Subunit counting in membrane-bound proteins. *Nat Methods* 4:319–321.
4. Luik RM, Wu MM, Buchanan J, Lewis RS (2006) The elementary unit of store-operated Ca^{2+} entry: local activation of CRAC channels by STIM1 at ER-plasma membrane junctions. *J Cell Biol* 174:815–825.
5. Xu P, *et al.* (2006) Aggregation of STIM1 underneath the plasma membrane induces clustering of Orai1. *Biochem Biophys Res Commun* 350:969–976.
6. Wu MM, Buchanan J, Luik RM, Lewis RS (2006) Ca^{2+} store depletion causes STIM1 to accumulate in ER regions closely associated with the plasma membrane. *J Cell Biol* 174:803–813.
7. Betzig E, *et al.* (2006) Imaging intracellular fluorescent proteins at nanometer resolution. *Science* 313:1642–1645.
8. Li Z, *et al.* (2007) Mapping the interacting domains of STIM1 and Orai1 in Ca^{2+} release-activated Ca^{2+} channel activation. *J Biol Chem* 282:29448–29456.
9. Grynkiewicz G, Poenie M, Tsien RY (1985) A new generation of Ca^{2+} indicators with greatly improved fluorescence properties. *J Biol Chem* 260:3440–3450.
10. Chen L, Koh DS, Hille B (2003) Dynamics of calcium clearance in mouse pancreatic β-cells. *Diabetes* 52:1723–1731.

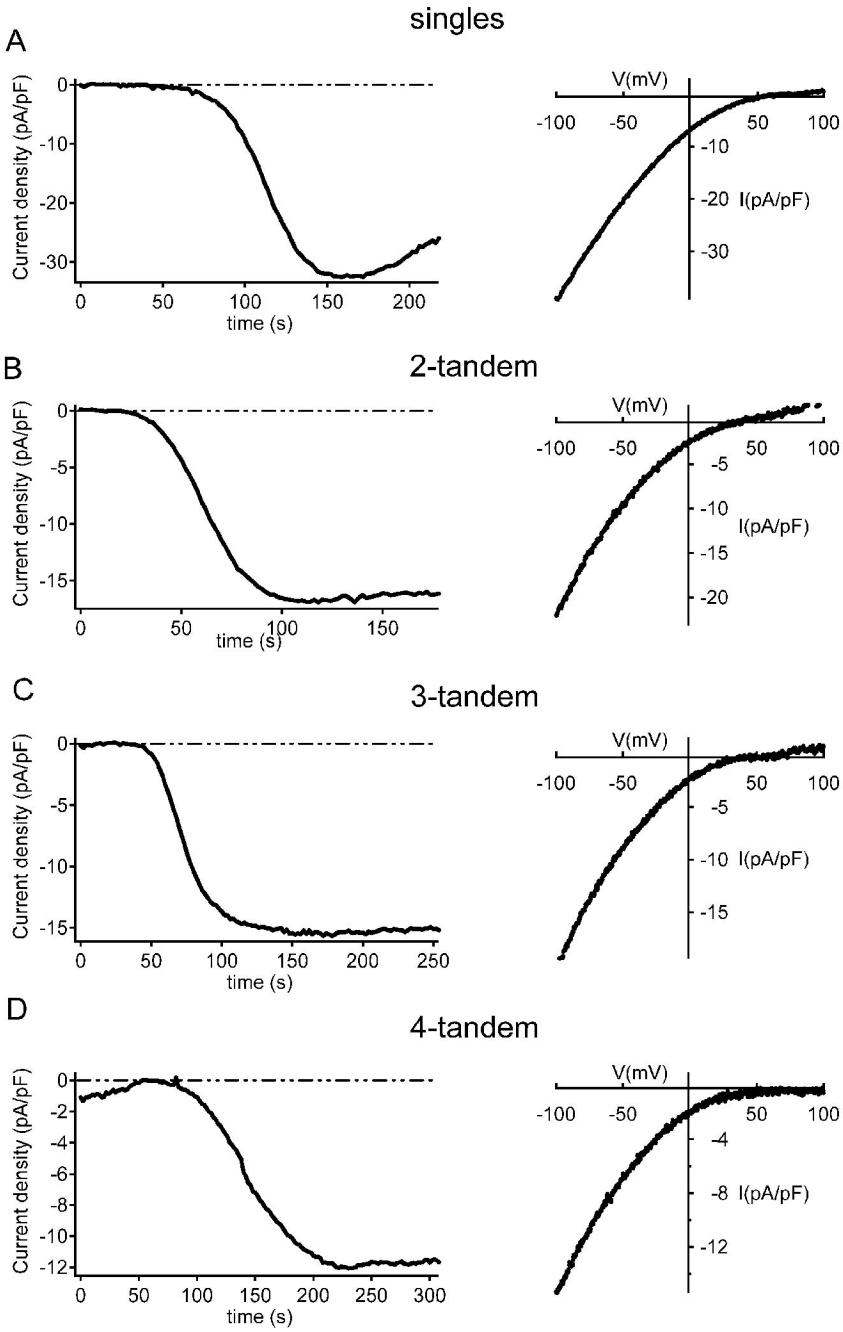

Fig. S1. Coexpressing STIM1–mOrange with any Orai1 vector reconstituted large CRAC currents in HEK293 cells. After establishment of a whole-cell patch clamp, the CRAC channels in HEK293 cells were activated by passive ER depletion via intracellular perfusion of 12 mM BAPTA. The amplitude of the current recorded at −80 mV was used to monitor the development of CRAC current (I_{CRAC}). Representative time courses and current/voltage relationships obtained from cells transfected with Orai1 singles (*A*), two-tandem (*B*), three-tandem (*C*), and four-tandem (*D*) are shown here. Each trace is representative of at least five similar experiments except that the current magnitude varied considerably from cell to cell.

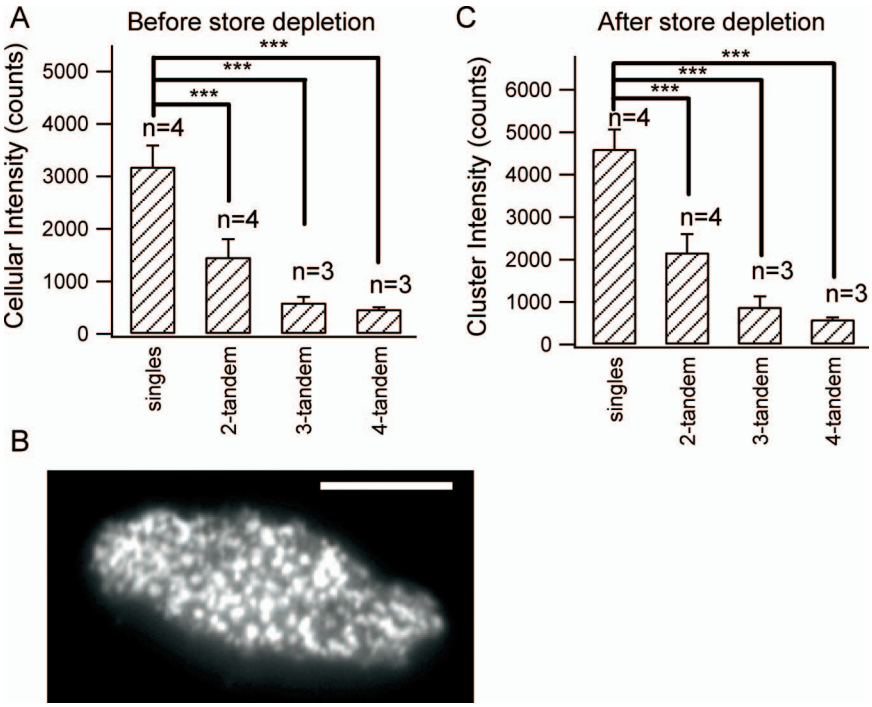

Fig. S2. Relative surface expression of the different Orai1 constructs. HEK293 cells were cotransfected with STIM-3xFLAG-SBP-CBP and Orai1–EGFP constructs. Images were captured from fixed cells at a gain 100-fold lower than that used in the single-molecule imaging experiments in Fig. 1. Therefore, 1,000 counts corresponds to 3,500 photons in *A* and *C*. (*A*) The average fluorescence intensity of EGFP at the plasma membrane is measured in quiescent cells under a TIRF microscope. Numbers of cells tested and results of the significance test are labeled on the graph (***$P < 0.001$). (*B*) After depletion of ER calcium stores with TG (1 μM) for >10 min, Orai1 formed clusters of relatively uniform intensity (Scale bar, 10 μm.) (*C*) Fluorescence intensity of clusters after store depletion. Numbers of cells tested and results of significance test are labeled on the graph (***$P < 0.001$).

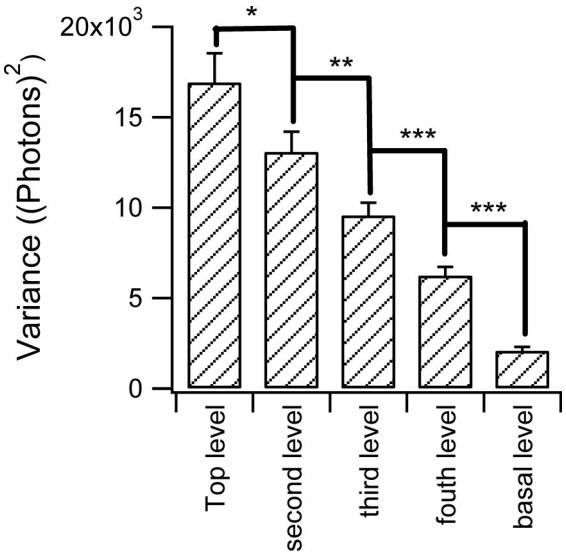

Fig. S3. Fluctuations in the fluorescence intensity correlate with the numbers of EGFP molecules remaining. The variance of the fluorescence intensity is plotted against the level number for four steps of bleaching in fixed cells expressing Orai1–EGFP singles. Results of paired *t* tests are labeled on the graph (*$P < 0.05$; **$P < 0.01$; ***$P < 0.001$).

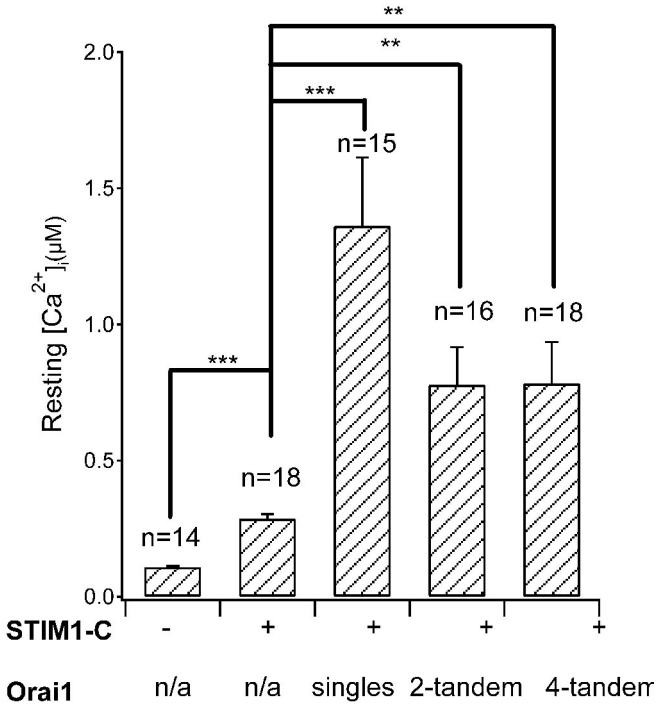

Fig. S4. Significantly elevated $[Ca^{2+}]_i$ in live cells transfected with either STIM1-C–mCherry alone or cotransfected with STIM1-C–mCherry and different EGFP-tagged Orai1 vectors. (*$P < 0.05$; **$P < 0.01$; ***$P < 0.001$).

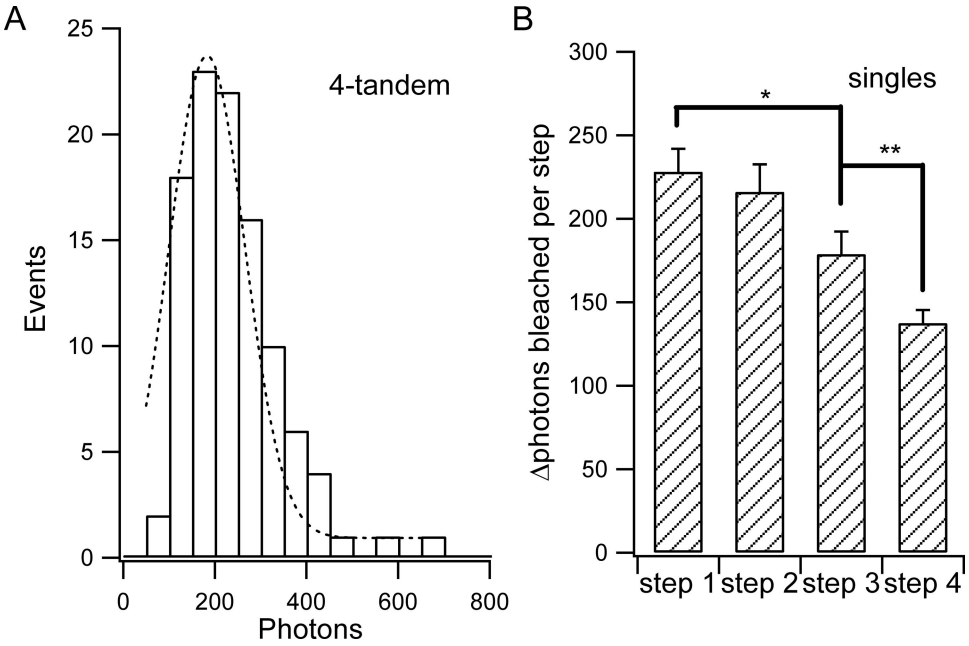

Fig. S5. Amplitude analysis of bleaching steps. (*A*) The fluorescence intensity measured from bleaching steps of Orai1 four-tandems tagged with EGFP exhibited a nearly Gaussian distribution (dashed line) with a midpoint at 183 ± 7 photons ($n = 104$). (*B*) Mean bleaching steps for Orai1 singles showed a trend during four steps of bleaching. The first bleaching step was somewhat larger than the last two ($n = 60$). Results of paired *t* tests are labeled on the graph (*$P < 0.05$; **$P <$ 0.01).

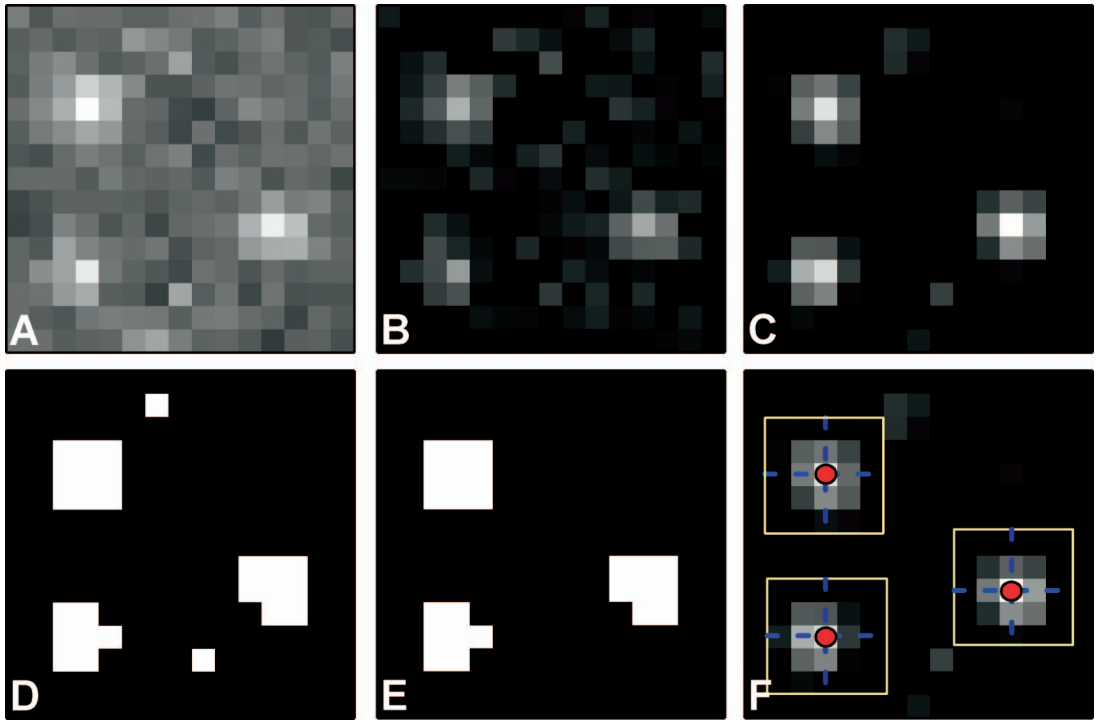

Fig. S6. Algorithm for determination of the center of the fluorescent spots. An example raw image is shown in *A*. Five similar frames were averaged (*B*) and then filtered to remove background noise (*C*). The image was thresholded thereafter to determine the areas of fluorescence spots (*D*), and was filtered again to eliminate discrete pixels not associated with cellular materials (*E*). Finally, we selected the brightest pixel of each punctum as the exact center position (red spot), and enclosed each spot with a square of 5 × 5 pixels for subsequent analysis of fluorescence intensity (*F*). The image resolution is 160 nm/pixel.

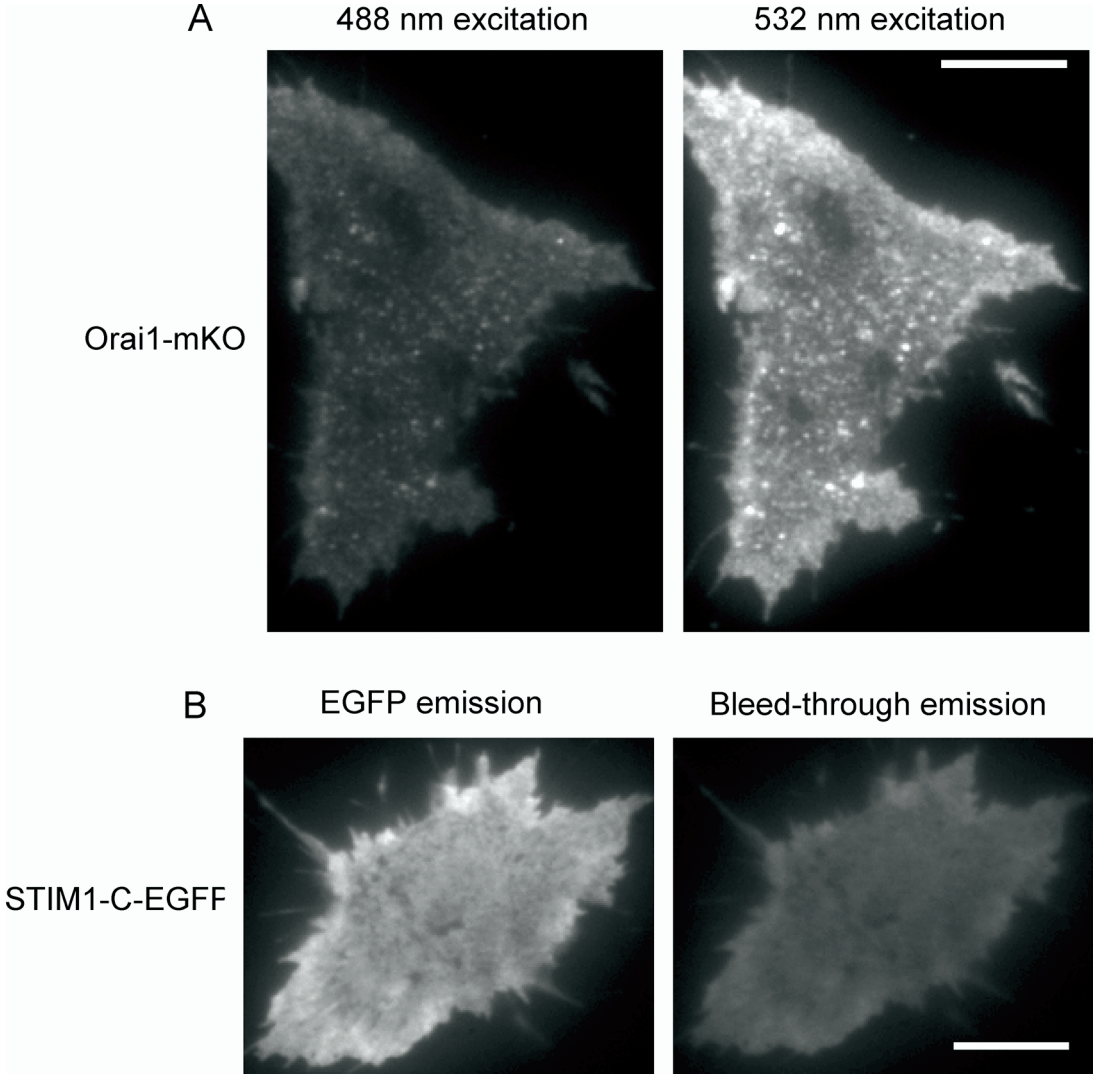

Fig. S7. Calibration of the sensitized emission method to measure FRET. (*A*) Live HEK293 cells expressing only Orai1–mKO as observed under TIRF microscopy. The intensity of mKO fluorescence when excited by the 488-nm laser (cross-excitation) was 34% of the value when excited by the 532-nm laser. (*B*) Live HEK293 cells expressing only STIM1-C–EGFP and excited by 488-nm laser as observed under TIRF microscopy. The EGFP emission recorded in the mKO emission channel (bleed-through) was 43% of the emission in the GFP channel. (Scale bars, 10 μm.)